Topics in associated $J/\psi + c + \bar{c}$ production at modern colliders

S. P. Baranov*

P. N. Lebedev Institute of Physics, Leninsky prosp. 53, Moscow 119991, Russia

(Received 9 February 2006; revised manuscript received 11 April 2006; published 27 April 2006)

In the framework of perturbative QCD and nonrelativistic bound state formalism, we calculate the production of J/ψ mesons associated with open-charm particles at HERA and Tevatron conditions. We show that the contribution from $J/\psi + c + \bar{c}$ channel becomes comparable with that of J/ψ sole production at high J/ψ transverse momenta (approximately, at $p_{\psi,T} > 10$ GeV). We investigate the J/ψ polarization effects and kinematic correlations between J/ψ mesons and the accompanying open-charmed mesons. We show that the correlations are sensitive to the initial k_t of the colliding partons, and so, can be considered as an additional test discriminating the collinear parton model and the k_t-factorization approach.

DOI: 10.1103/PhysRevD.73.074021 PACS numbers: 12.38.Bx, 13.85.Ni

I. INTRODUCTION

Compared to the inclusive inelastic J/ψ production, only little attention is paid in the literature to the associated production of J/ψ mesons with open-charm particles. The aim of the present study is to fill this gap. In this paper we are going to show that the production cross section of $J/\psi + c + \bar{c}$ states is not too small, and so, the process not only can be detected, but even the properties of inclusive J/ψ production cannot be properly understood without taking the $J/\psi + c + \bar{c}$ channel into account. Furthermore, we show that the considered process is connected with rich underlying physics. In particular, the interparticle kinematic correlations can shed more light on the internal parton dynamics in the colliding hadrons.

The outline of the paper is the following. In Sec. II we briefly describe the theoretical grounds of our calculations. One of the goals of the present paper is to compare the predictions on the charm-associated and individual J/ψ production. Therefore, we find it helpful to recall the J/ψ production schemes, and we do that in Sec. III. In Sec. IV we display our numerical results and discuss the relevant physics. Our findings are summarized in Sec. V. The technical details of the calculations are presented in the appendix.

II. THEORETICAL FRAMEWORK

Our approach is based on three theoretical ingredients. These are the perturbative QCD, the nonrelativistic bound state formalism, and the k_t-factorization in the parton model. In this study we consider the photon-gluon and gluon-gluon fusion reactions, namely

$$\gamma + g \to J/\psi + c + \bar{c}, \tag{1}$$

$$g + g \to J/\psi + c + \bar{c}. \tag{2}$$

The full gauge invariant set comprises 24 and 36 Feynman diagrams in the cases of photon-gluon (1) and gluon-gluon (2) fusion, respectively. The relevant gluon-gluon fusion diagrams are displayed in Fig. 1. The explicit expressions for the corresponding matrix elements are presented in the appendix. The evaluation of the diagrams is straightforward and follows the standard Feynman rules. Technically, the computations are organized according to the orthogonal amplitudes method described in detail in Ref. [1]. The calculation of traces is performed using the algebraic manipulation system REDUCE [2].

When calculating the spin average of the matrix element squared, we substitute the full lepton tensor for the photon polarization matrix:

$$\overline{\epsilon_\gamma^\mu \epsilon_\gamma^{*\nu}} = [4p_e^\mu p_e^\nu - 2(p_e k_\gamma) g^{\mu\nu}]/(k_\gamma^2), \tag{3}$$

where p_e is the initial electron momentum and k_γ the photon momentum. The form of the gluon spin density matrix is different depending on whether the gluon is on shell (as is assumed in the conventional parton model) or off shell (in the k_t-factorization approach). For the general case, we adopt the k_t-factorization prescription [3–5]:

$$\overline{\epsilon_g^\mu \epsilon_g^{*\nu}} = p_p^\mu p_p^\nu x_g^2/|k_T|^2 = k_T^\mu k_T^\nu/|k_T|^2, \tag{4}$$

where p_p is the initial proton momentum, x_g the gluon momentum fraction, k_T the component of the gluon momentum perpendicular to the beam axis, and the bar stands for the averaging over the gluon spin. In the collinear limit, when $k_T \to 0$, this expression converges to the ordinary $\overline{\epsilon_g^\mu \epsilon_g^{*\nu}} = -\frac{1}{2} g^{\mu\nu}$.

The J/ψ polarization vector ϵ_ψ is defined as an explicit four-vector. In the frame where the z axis is oriented along the J/ψ momentum vector, $p_\psi = (0, 0, |p_\psi|, E_\psi)$, the polarization vector reads for different helicity states

$$\begin{aligned} \epsilon_{\psi(\pm 1)} &= (1, \pm i, 0, 0)/\sqrt{2}, \\ \epsilon_{\psi(0)} &= (0, 0, E_\psi, |p_\psi|)/m_\psi. \end{aligned} \tag{5}$$

*Email address: baranov@sci.lebedev.ru

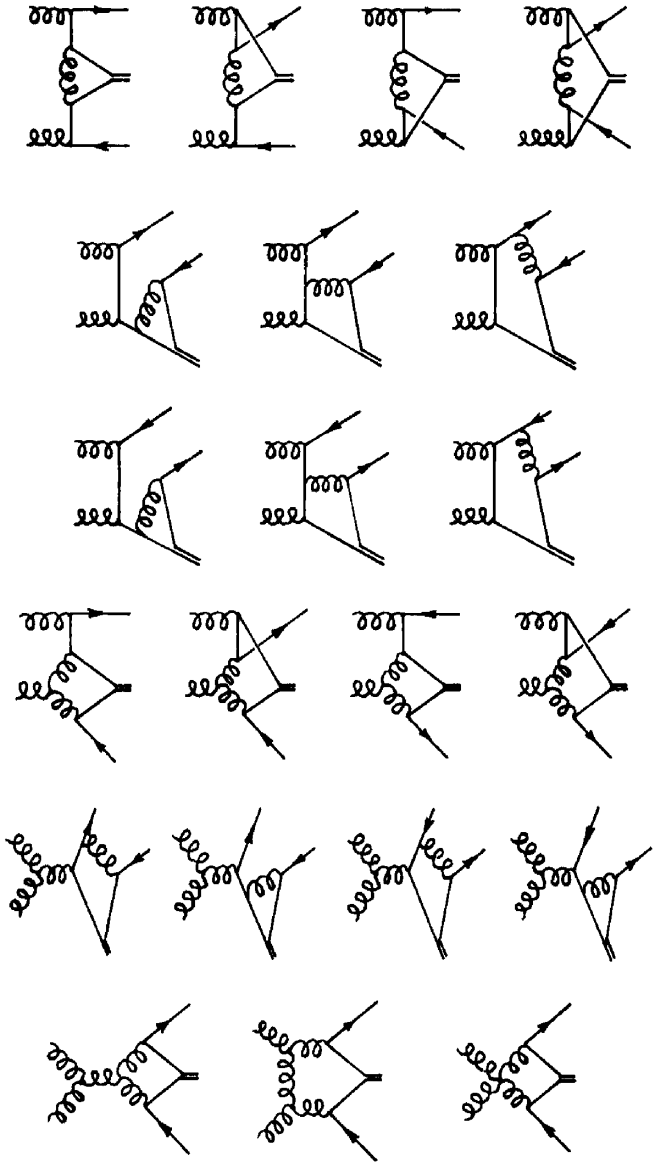

FIG. 1. Feynman diagrams representing the subprocess $g + g \to J/\psi + c + \bar{c}$.

As we believe that the formation of J/ψ state is dominated by the color-singlet mechanism [6], we do not take into account the possible color-octet contributions. In fact, we have already demonstrated [7,8] that the color-singlet model alone (considered in the framework of the k_t-factorization approach) successfully describes the available data on the inclusive J/ψ production both at the Tevatron and HERA. Then, the J/ψ formation probability reduces to the only parameter $|\Psi(0)|^2$, the value of wave function at the origin of coordinate space, which is known from the J/ψ leptonic decay width [9].

The multiparticle phase space $\prod d^3p_i/(2E_i)\delta^4(\sum p_{\text{in}} - \sum p_{\text{out}})$ of the reactions $e + p \to J/\psi + c + \bar{c} + X$ and $p + p \to J/\psi + c + \bar{c} + X$ is parametrized in terms of rapidities, transverse momenta, and azimuthal angles: $d^3p_i/(2E_i) = (\pi/2)dp_{iT}^2 dy_i d\phi_i/(2\pi)$. Let s be the total initial invariant energy squared, $\hat{s}$ the squared energy of the partonic subprocess, k_{1T}, k_{2T}, ϕ_1, and ϕ_2 the transverse momenta and azimuthal angles of the initial (off shell) partons, y_ψ, y_c, $y_{\bar{c}}$, $p_{\psi T}$, p_{cT}, $p_{\bar{c}T}$, ϕ_ψ, ϕ_c, and $\phi_{\bar{c}}$ the rapidities, transverse momenta, and azimuthal angles of J/ψ meson and the accompanying charmed quark and antiquark, respectively. Then, the fully differential cross section reads

$$\begin{aligned} d\sigma(pp \to \psi c\bar{c}X) &= \frac{\pi\alpha_s^4}{3\hat{s}^2}|\Psi(0)|^2 \frac{1}{4}\sum_{\text{spins}}\frac{1}{64}\sum_{\text{colors}}|\mathcal{M}(gg \to \psi c\bar{c})|^2 \\ &\times \mathcal{F}_g(x_1, k_{1T}^2, \mu^2)\mathcal{F}_g(x_2, k_{2T}^2, \mu^2)dk_{1T}^2 dk_{2T}^2 \\ &\times dp_{\psi T}^2 dp_{cT}^2 dy_\psi dy_c dy_{\bar{c}} \frac{d\phi_1}{2\pi}\frac{d\phi_2}{2\pi}\frac{d\phi_\psi}{2\pi}\frac{d\phi_c}{2\pi}. \end{aligned} \tag{6}$$

In this expression, $\mathcal{F}_g(x_i, k_{iT}^2, \mu^2)$ are the so-called unintegrated gluon distribution functions. They obey Balitsky-Fadin-Kuraev-Lipatov (BFKL) [10] or Catani-Ciafaloni-Fiorani-Marchesini (CCFM) [11] equations and reduce to the conventional parton densities $G(x, \mu^2)$ once the k_T dependence is integrated out:

$$\int_0^{\mu^2} \mathcal{F}(x, k_T^2, \mu^2)dk_T^2 = xG(x, \mu^2). \tag{7}$$

In order to estimate the degree of theoretical uncertainty connected with the choice of unintegrated gluon density, we use two different parametrizations, which are known to show the largest difference with each other, namely, the ones proposed in Refs. [3,12]. In the first case [3], the unintegrated gluon density is derived from the ordinary (collinear) density $G(x, \mu^2)$ by differentiating it with respect to μ^2 and setting $\mu^2 = k_T^2$. In the approach of [12], the unintegrated density is calculated as the convolution of the ordinary gluon density with some universal weight factor. In both cases we use the LO Glück-Reya-Vogt (GRV) set [13] as the input collinear density. This set is also used to show the predictions of collinear parton model.[1]

The initial parton momentum fractions x_1 and x_2 are calculated from the independent integration variables using the energy-momentum conservation laws in the light cone projections:

$$\begin{aligned} (k_1 + k_2)_{E+p_\parallel} &= x_1\sqrt{s} \\ &= m_{\psi T}\exp(y_\psi) + m_{cT}\exp(y_c) \\ &\quad + m_{\bar{c}T}\exp(y_{\bar{c}}), \end{aligned} \tag{8}$$

[1]Then we omit the integration over k_{1T}^2 and k_{2T}^2 in Eq. (6) and use the on shell expression for the gluon-gluon fusion matrix element $|\mathcal{M}(gg \to \psi c\bar{c})|^2$.

$$(k_1 + k_2)_{E-p_{||}} = x_2\sqrt{s} = m_{\psi T}\exp(-y_\psi) + m_{cT}\exp(-y_c) + m_{\bar{c}T}\exp(-y_{\bar{c}}), \quad (9)$$

with $m_{iT} = (m_i^2 + |p_{iT}|^2)^{1/2}$, $i = \psi, c, \bar{c}$. The phase space physical boundary is determined by the inequalities

$$G(\hat{s}, \hat{t}_1, \hat{s}_2, k_1^2, k_2^2, m_c^2) \leq 0, \quad (10)$$

$$(m_c + m_\psi)^2 \leq \hat{s}_2 \leq (\sqrt{\hat{s}} - m_c)^2, \quad (11)$$

where $\hat{s} = (k_1 + k_2)^2$, $\hat{t}_1 = (k_1 - p_c)^2$, $\hat{s}_2 = (p_\psi + p_{\bar{c}})^2$, and G is the standard kinematic function [14]. The multidimensional integration in (6) has been performed by means of the Monte Carlo technique, using the routine VEGAS [15]. Finally, to convert the charmed quark and antiquark into real physical states (say, D-mesons) we use Peterson [16] fragmentation function with $\epsilon = 0.06$. The fragmentation probability is set equal to 1 (it means that, in fact, we collect the cross section corresponding to all possible charmed states). The full FORTRAN code used in the calculations is available from the author on request.

III. k_t-FACTORIZATION VERSUS COLLINEAR TREATMENT OF J/ψ PRODUCTION

One of the goals of the present paper is to compare the predictions on the charm-associated and nonassociated J/ψ production. Therefore, we find it helpful to recall the J/ψ production schemes employed in the collinear and k_t-factorization approaches.

The lowest order diagram consistent with all quantum number conservation laws is presented in Fig. 2(a). Naively, it ought to make the dominant contribution, but, when considered in the collinear factorization framework, it shows too steep falloff with increasing $p_{\psi,T}$ being at odds with experimental data. The theory is then "repaired" by attributing the production cross section to another, the so-called "color-octet" mechanism [17], depicted in Fig. 2(b). Although the emission of soft final-state gluons is treated here in a nonperturbative way, this scheme can be regarded as an effective $\mathcal{O}(\alpha_s^5)$ process. On the other hand, the color-octet mechanism is not equivalent to the true $\mathcal{O}(\alpha_s^5)$ QCD calculations, because it only focuses on a specific single diagram of Fig. 2(b) [which is made dominant due to a special choice of phenomenological matrix elements], while all the other possible contributions, like the ones shown in Fig. 2(c), are ignored.

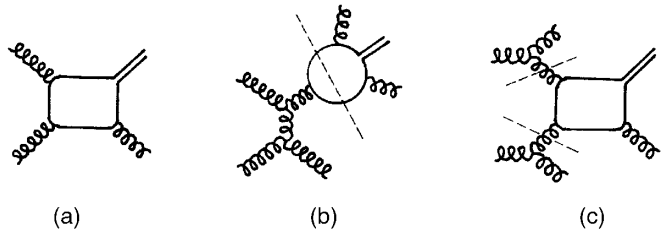

FIG. 2. Diagrams representing J/ψ production subprocesses. (a) Leading-order gluon-gluon fusion. (b) Color-octet scheme. Part of the diagram to the right of the dashed line is treated in a nonperturbative way: the emission of soft gluons is absorbed into phenomenological color-octet matrix elements. (c) Higher-order contributions connected with initial gluon radiation. In the k_t-factorization approach, the upper and the lower parts of this diagram are included in the k_T evolution of gluon densities.

The p_T dependence of the cross section is determined by the t-channel gluon propagator in the hard partonic subprocess ($g + g \to g + g^*$), and thus, is $d\sigma/dp_{\psi,T} \sim 1/p_{\psi,T}^4$, in agreement with the data. At $p_{\psi,T} \gg m_\psi$, the fragmenting gluon g^* is nearly on shell, and so, must possess strong transverse polarization. The latter prediction is not supported by the data.

In the k_t-factorization approach, the natural hierarchy of the matrix elements is restored. The dominant contribution comes from the lowest order diagram of Fig. 2(a). As soon as the initial gluon k_T is taken into account, the broadening effect makes the shape of the J/ψ spectrum fully consistent with the data. The integrated cross section does not change much in comparison with $\mathcal{O}(\alpha_s^3)$ collinear calculations, but it is only redistributed over a broader $p_{\psi,T}$ range. The p_T dependence of the cross section is now determined by the behavior of the unintegrated gluon density, which shows $d\sigma/dp_{\psi,T} \sim 1/p_{\psi,T}^4$. This behavior can be related to the t-channel gluon propagators in the "ladder" diagrams describing the k_T evolution of gluon density.

In fact, the evolution of gluon densities takes into account a large piece of higher-order corrections [like those shown in Fig. 2(c)], collecting the terms of the type $[\alpha_s \ln(1/x)]^n$ and $[\alpha_s \ln(\mu^2/\Lambda^2)\ln(1/x)]^n$ up to infinitely large n (see [3]). Thanks to that, the calculations employing the leading-order partonic matrix elements can show effects, which are known in collinear calculations with next-to-leading order (NLO) matrix elements.

It is important that the initial gluon transverse momentum leads to gluon off shellness and, consequently, to the presence of longitudinal components in the gluon polarization vector. This property plays the key role in understanding the J/ψ polarization phenomenon. Typically, the k_T values of the two colliding gluons are much different, as the parton evolution is equivalent to the random walk in the $\ln|k_T|$ plane, not in the k_T plane. Roughly speaking, the k_T of one of the gluons can be neglected in comparison with that of the other. So, in the initial state there is one nearly on shell (transversely polarized) gluon and one off shell (longitudinally polarized) gluon. After the interaction, they convert into one on shell (transversely polarized) gluon and a heavy vector meson. Simple helicity conservation arguments show that the polarization of vector meson must be longitudinal, in contrast with the ordinary parton model, where the initial gluons are both on shell.

The reader may have trouble about the discrepancy between the collinear and k_t-factorization predictions. The difference originates from the fact that the calculations are based on completely different sets of Feynman diagrams. It is possible to say that, in this particular case, the observed difference is not between the collinear and k_t-factorization interpretations of QCD, but is rather between the full LO + NLO pQCD and the color-octet model prescriptions. At present, there is no full LO + NLO collinear calculation for the hadronic production of J/ψ mesons, but there is such a calculation for photonic J/ψ production [18]. It demonstrates that the difference between the collinear LO and k_t-factorization results is rather significant, but including the NLO contribution makes the collinear results much closer to the k_t-factorization predictions.

This fact seems reasonable and understandable, because the intermediate gluons in the NLO diagrams [internal lines in Fig. 2(c)] bear strong resemblance to the initial gluons in the k_t-factorization approach in Fig. 2(a): they are off shell, carry transverse momentum, etc. At the same time, the color-octet model seems to attribute an inadequately large role to the diagram of Fig. 2(b). It is worth saying once again that the situation with J/ψ is exceptional, and when the calculations are based on the same set of Feyman diagrams (e.g., the case of $J/\psi + c + \bar{c}$ process) the difference between the two approaches should not be very dramatic.

IV. NUMERICAL RESULTS AND DISCUSSION

The numerical results are displayed in Figs. 3–8. First, we consider the Fermilab Tevatron conditions. In calculations, we set the total center of mass system (c.m.s.) energy $\sqrt{s} = 1800$ GeV, the charmed quark mass $m_c = m_\psi/2 = 1.55$ GeV, the factorization and renormalization scales $\mu_F^2 = \mu_R^2 = \hat{s}/4$, we use the LO GRV [13] collinear gluon density in the proton and two different sets of unintegrated gluon densities described in Refs. [3,12].

The most important theoretical uncertainty in the overall production rates is connected with the choice of remormalization scale μ_R in the strong coupling constant: note that the cross section (6) is proportional to the fourth power of α_s. Variations in μ_R from $\mu_R^2 = \hat{s}$ to $\mu_R^2 = \hat{s}/4$ change the cross section by a factor of 2. The sensitivity of the ratio $\sigma(\psi cc)/\sigma(\psi)$ is much lower, because three powers of α_s cancel out. The sensitivity of the results to the factorization scale μ_F is nearly the same in the k_t-factorization and collinear calculations. Variations in μ_F from $\mu_F^2 = \hat{s}$ to $\mu_F^2 = \hat{s}/4$ change the cross section by a factor of 1.25.

The choice of unintegrated gluon density has a significant effect on the p_T distributions and azimuthal correlations. The parametrizations [3,12] used in our calculations are known to show the largest difference with each other, and so, to some extent, they outline the theoretical uncertainty band.

We begin the discussion with showing the transverse momentum distributions $d\sigma/dp_T$ for J/ψ mesons and the accompanying charmed mesons in Fig. 3. The presence of the initial gluon transverse momentum (in the

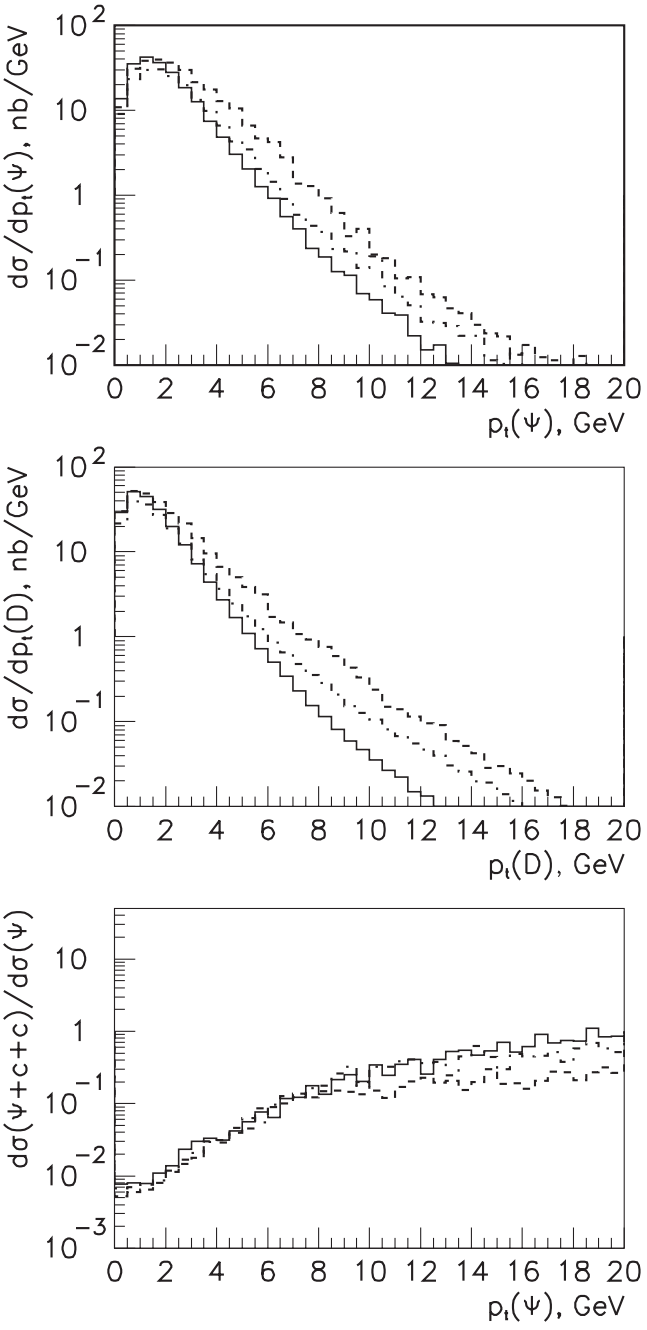

FIG. 3. $J/\psi + c + \bar{c}$ production at the Tevatron. Upper panel: J/ψ transverse momentum distribution; middle panel: charmed meson transverse momentum distribution; lower panel: the ratio of the $J/\psi + c + \bar{c}$ production cross section to the noncharm-associated J/ψ production. Solid histograms: predictions of the collinear parton model; dashed and dash-dotted histograms: k_t-factorization approach with JB [12] and dGRV [3] gluon densities, respectively.

k_t-factorization approach) leads to the p_T-broadening effect, which is stronger for JB [12] gluon density than for dGRV [3] density.

We find it interesting to compare the production rates of J/ψ mesons appearing as individual particles (i.e. without coproduced charm) and in association with open-charmed states. The production of individual J/ψ particles can proceed via the color-singlet and color-octet channels. In the collinear factorization scheme, the high-p_T region is dominated by the color-octet contribution. The latter is characterized by the behavior $d\sigma/dp_{\psi,T} \sim 1/p^4_{\psi,T}$, as it was explained in the previous section. In the k_t-factorization approach, one only has to take into account the color-singlet contribution [7]. In this case, the matrix element of the process $g + g \to J/\psi + g$ is strongly peaking in the forward direction, and the p_T dependence of the cross section is determined by the behavior of the unintegrated gluon density, which shows $d\sigma/dp_{\psi,T} \sim 1/p^4_{\psi,T}$.

The dominant contribution to the associated $J/\psi + c + \bar{c}$ production at high $p_{\psi,T}$ comes from the quark fragmentation diagrams: $g + g \to c + \bar{c}$, $c \to J/\psi + c$, as it was demonstrated in Ref. [19]. Here, the p_T dependence of the cross section is determined by the hard partonic subprocess $g + g \to c + \bar{c}$, resulting in $d\sigma/dp_{\psi,T} \sim 1/p^4_{\psi,T}$. This holds for both the collinear and k_t-factorization approaches, as the initial gluon transverse momentum follows the same law and $\mathcal{O}(1/p^4_{\psi,T}) + \mathcal{O}(1/p^4_{\psi,T}) = \mathcal{O}(1/p^4_{\psi,T})$.

Thus, we see that the asymptotic powerlike behavior is universal for the production of charm-associated and individual J/ψ mesons, both in the collinear and k_t-factorization approaches. In accord with that, the ratio of the differential cross sections $r = [d\sigma(\psi c\bar{c})/dp_{\psi,T}]/[d\sigma(\psi)/dp_{\psi,T}]$ flattens at high $p_{\psi,T}$ tending to a constant value. The numerical value of this constant depends on the matrix elements of the relevant partonic subprocesses and turns out to be of the order of $1/3$.

The color coefficients give at least partial explanation for the fact that the ratio of the cross sections is not small. Consider this point in more detail. The individual J/ψ production subprocess $g + g \to J/\psi + g$ is represented by the color structure

$$\mathcal{M}^{\rm col}_{\psi} = \mathrm{tr}\{T^a T^b T^c\} = (1/4)d^{abc} + (i/4)f^{abc}. \quad (12)$$

The color-antisymmetric coupling f^{abc} is C-even, and so, is inconsistent with charge parity conservation because J/ψ is a C-odd state. Hence, we are left with d^{abc} coupling only, which gives after squaring

$$|\mathcal{M}^{\rm col}_{\psi}|^2 = (1/16)d^{abc}d^{abc} = 5/6. \quad (13)$$

This has to be compared with the diagrams $\mathcal{M}_{21}$, $\mathcal{M}_{31}$, $\mathcal{M}_{51}$, and $\mathcal{M}_{53}$ (the first diagram in the second and the third rows, the second and the fourth diagrams in the fifth row in Fig. 1) responsible for the associated $J/\psi + c + \bar{c}$ production in the fragmentation limit. The relevant expressions for their color structure (see Appendix) can be rewritten as

$$\begin{aligned}\mathcal{M}^{\rm col}_{21} &= (T^a T^b T^c T^c)^{\alpha}_{\beta} \\ &= (2/9)\delta^{ab} I^{\alpha}_{\beta} + (2/3) i f^{abc} (T^c)^{\alpha}_{\beta} \\ &\quad + (2/3) d^{abc} (T^c)^{\alpha}_{\beta} \end{aligned} \quad (14)$$

and

$$\mathcal{M}^{\rm col}_{51} = (T^c T^d T^d)^{\alpha}_{\beta} i f^{abc} = (4/3) i f^{abc} (T^c)^{\alpha}_{\beta}. \quad (15)$$

They give after squaring

$$\begin{aligned}|\mathcal{M}^{\rm col}_{21}|^2 &= |\mathcal{M}^{\rm col}_{31}|^2 = (32/27) + (16/3) + (80/27) \\ &= 256/27 \end{aligned} \quad (16)$$

and

$$|\mathcal{M}^{\rm col}_{51}|^2 = |\mathcal{M}^{\rm col}_{53}|^2 = 64/3. \quad (17)$$

These numbers are a factor of 10 to 20 larger than the color coefficient in Eq. (13).

We proceed with showing the rapidity distributions of J/ψ mesons and the coproduced charmed mesons in Fig. 4.

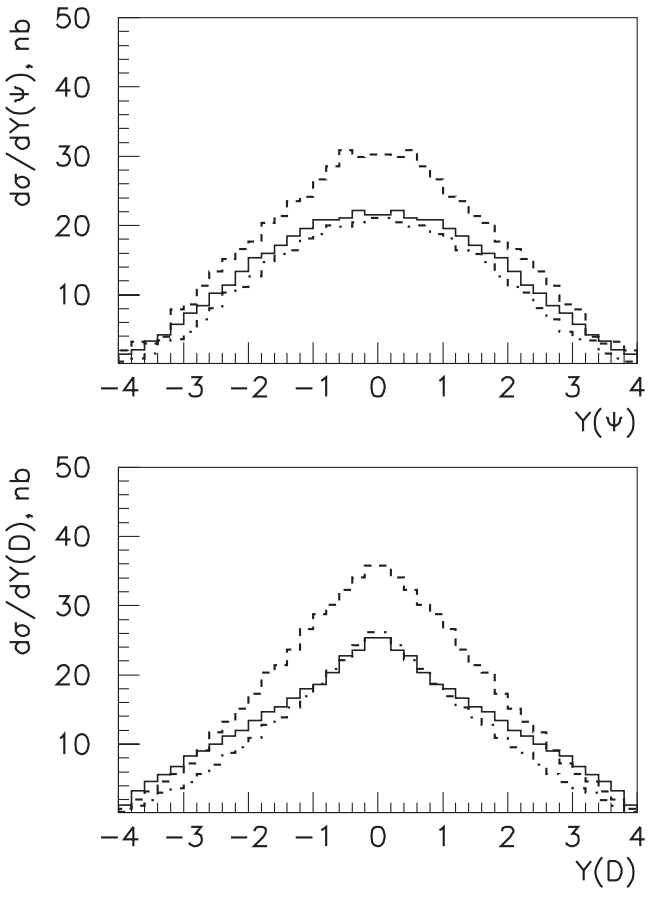

FIG. 4. $J/\psi + c + \bar{c}$ production at the Tevatron. J/ψ and charmed meson rapidity distributions. Notation of the curves is as in Fig. 3.

The distributions obtained with different parametrizations of gluon densities are all similar in shape and only differ in the total normalization.

Next, we focus attention on the interparticle correlations. Figure 5 displays the distributions in $\Delta\varphi$, the azimuthal angle between the J/ψ and the coproduced charmed meson momenta, $\Delta\eta$, the rapidity difference, and the variable R defined as $\Delta R = \sqrt{\Delta\varphi^2 + \Delta\eta^2}$. One can see that the initial gluon transverse momentum has quite a significant effect on the azimuthal correlations. As the average initial gluon k_T increases, the $\Delta\varphi$ distribution moves steadily from $\Delta\varphi \simeq \pi$ towards $\Delta\varphi \simeq 0$. This effect is due to nothing but kinematics. In the gluon-gluon center-of-mass system, the angular distributions look like in the collinear parton model, but when we consider them in a

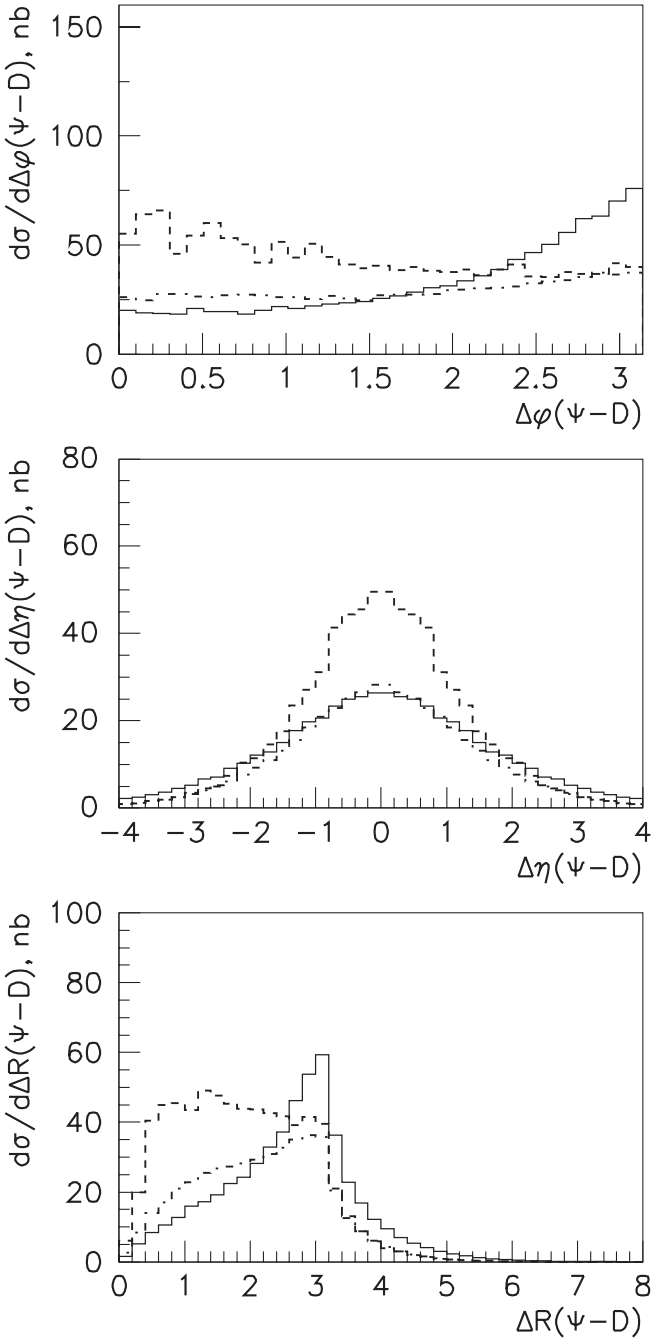

FIG. 5. $J/\psi + c + \bar{c}$ production at the Tevatron. Kinematic correlations between the J/ψ and accompanying charmed mesons. Upper panel: azimuthal angle difference; middle panel, pseudorapidity difference; lower panel: combined variable $\Delta R = \sqrt{(\Delta\varphi)^2 - (\Delta\eta)^2}$. Notation of the curves is as in Fig. 3.

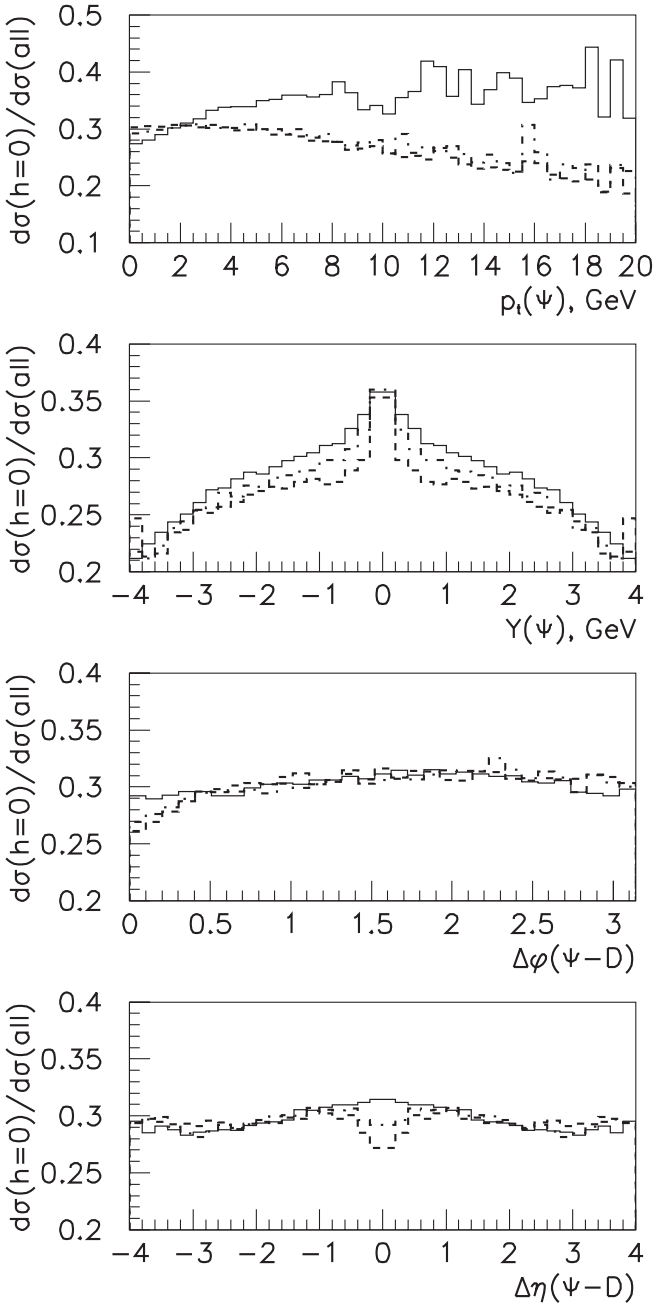

FIG. 6. $J/\psi + c + \bar{c}$ production at the Tevatron. The fraction of longitudinally polarized J/ψ mesons as a function of J/ψ transverse momentum, J/ψ rapidity, $J/\psi - D$ azimuthal angle difference, and $J/\psi - D$ pseudorapidity difference, from top to bottom, respectively. Notation of the curves is as in Fig. 3.

system moving in the transverse direction the azimuthal angles between particles become smaller. Hence, the shape of the $\Delta\varphi$ distribution measures the average k_T of the colliding gluons. It not only can distinguish the k_t-factorization approach from the collinear parton model, but even discriminate the different unintegrated gluon densities.

Now, let us turn to polarization variables. Figure 6 displays the fraction of longitudinally polarized J/ψ mesons (the fraction of helicity $= 0$ states with respect to all possible polarizations) plotted as a function of $p_{\psi,T}$, η_ψ, $\Delta\varphi$, and $\Delta\eta$. In all cases, this fraction appears to be close to $1/3$, thus indicating that the mesons are, in essence, unpolarized.

This result is rather easy to believe in, because there are no special reasons for J/ψ mesons to be polarized. This contrasts with two-body partonic processes responsible for the production of individual J/ψ mesons. Note that the predictions of the k_t-factorization approach and collinear (color-octet) model on the polarization of individual J/ψ particles disagree with each other. If the dominant contribution comes from the gluon fragmentation into an octet $c\bar{c}$ pair, the mesons must have strong transverse polarization. On the contrary, if the production mechanism is the off shell gluon-gluon fusion, then the J/ψ polarization tends to be longitudinal, as it follows from simple helicity conservation arguments explained in Sec. III.

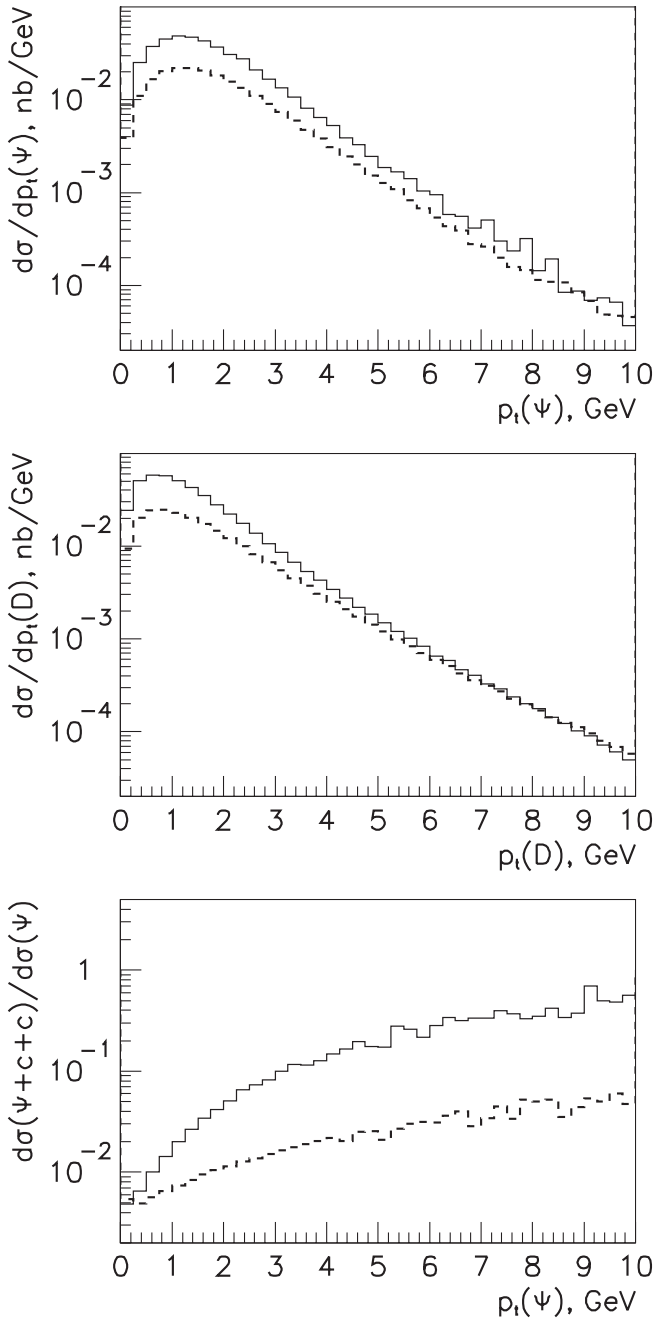

FIG. 7. $J/\psi + c + \bar{c}$ production at HERA. Upper panel: J/ψ transverse momentum distribution; middle panel, charmed meson transverse momentum distribution; lower panel: the ratio of the $J/\psi + c + \bar{c}$ production cross section to the noncharm-associated J/ψ production. Solid histograms: predictions of the collinear parton model; dashed histograms: k_t-factorization approach with JB [12] gluon densities.

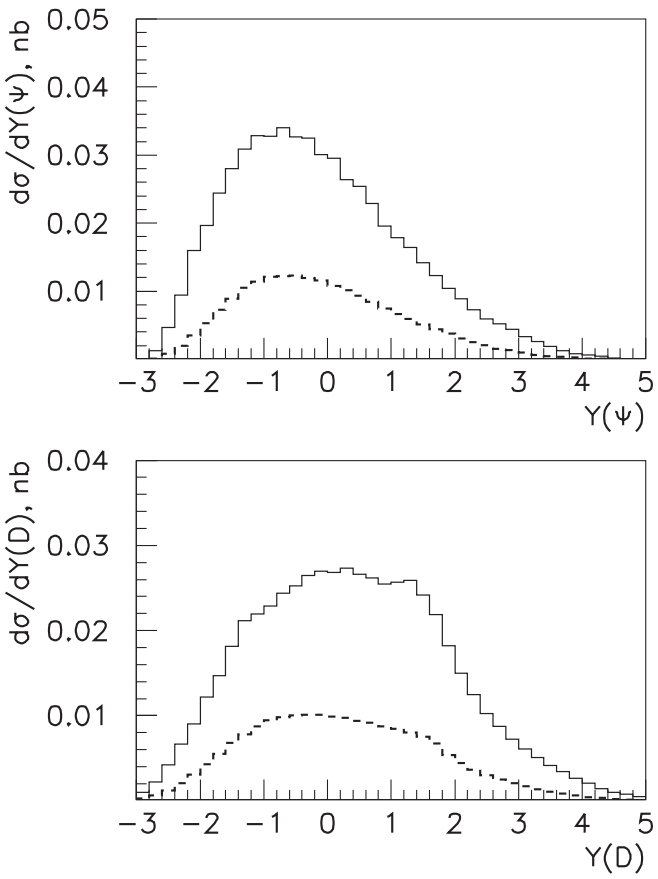

FIG. 8. $J/\psi + c + \bar{c}$ production at HERA. J/ψ and charmed meson rapidity distributions. Positive direction corresponds to the proton beam. Notation of the curves is as in Fig. 7.

None of these specific polarization mechanisms applies to the subprocess (2). In view of the fact that the charm-associated J/ψ production constitutes an important contribution to the total inelastic J/ψ production at high $p_{\psi,T}$, this contribution must have a significant effect on the overall measured J/ψ polarization.

The general regularities observed at the Tevatron conditions are also seen in ep collisions at HERA. However, in the latter case the production rates are much lower, and so, it looks almost hopeless to fulfil the polarization or correlation analysis. The only more or less realistic task could be to detect the process and estimate its cross section. The corresponding theoretical predictions are shown in Figs. 7 and 8.

V. CONCLUSION

We have considered the production of associated $J/\psi + c + \bar{c}$ states at the high energy colliders Tevatron and HERA. Our results can be summarized in three lessons. First, the associated production of J/ψ mesons with open-charm particles constitutes a significant fraction of the inclusive J/ψ production at high p_T. Asymptotically, the ratio of the production rates $\sigma(\psi c\bar{c})/\sigma(\psi)$ tends to a constant value of the order of $1/3$. Within the uncertainties coming from the choice of the renormalization and factorization scales and gluon distribution functions this quantity may range from $1/10$ to 1.

Second, the J/ψ mesons produced in association with open-charm states are practically unpolarized, and so, they contribute to the depolarization of the overall J/ψ sample. This is worth taking into account when analyzing the J/ψ polarization phenomenon at modern colliders.

Third, the azimuthal angular correlations between J/ψ mesons and the coproduced charmed particles are sensitive to the initial transverse momentum of the colliding gluons. This way, one can not only see the difference between the k_t-factorization approach and collinear parton model, but also discriminate the different unintegrated (k_T-dependent) gluon distributions. We conclude that the associated production of $J/\psi + c + \bar{c}$ states is an interesting and informative process connected with rich underlying physics.

ACKNOWLEDGMENTS

This work was supported by NATO Grant No. PST.CLG.980335.

APPENDIX

Let $k_1(\epsilon_1)$ and $k_2(\epsilon_2)$ be the 4-momenta (polarization vectors) of the incoming gluons; m_c and m_ψ the charmed quark and J/ψ meson masses; p_ψ the J/ψ momentum; p_1 and p_4 the momenta of the accompanying unbound charmed quark and antiquark; p_2 and p_3 the momenta of the charmed antiquark and quark forming the J/ψ meson; let also $k \equiv k_1 + k_2$. The nonrelativistic approximation implies $m_c = m_\psi/2$ and $p_2 = p_3 = p_\psi/2$.

The spin projection operator [6] $J_V = \epsilon\!\!\!/_\psi(p\!\!\!/_\psi + m_\psi)$ guarantees the proper quantum numbers of the $c\bar{c}$ bound state, i.e. $J^{\mathrm{PC}} = 1^{--}$ with ϵ_ψ being the polarization vector of J/ψ meson. Then, the matrix elements of the partonic subprocess reads

$$\mathcal{M}_{11} = \bar{u}(p_1)\epsilon\!\!\!/_1(p\!\!\!/_1 - k\!\!\!/_1 + m_c)\gamma_\mu J_V \gamma^\mu(k\!\!\!/_2 - p\!\!\!/_4 + m_c)\epsilon\!\!\!/_2 u(p_4)/[8(k_1p_1)(k_2p_4)(m_c^2 - k_1p_1 - k_1p_2 + p_1p_2)],$$
$$\mathcal{M}_{12} = \bar{u}(p_1)\gamma_\mu(k\!\!\!/_1 - p\!\!\!/_2 + m_c)\epsilon\!\!\!/_1 J_V \gamma^\mu(k\!\!\!/_2 - p\!\!\!/_4 + m_c)\epsilon\!\!\!/_2 u(p_4)/[8(k_1p_2)(k_2p_4)(m_c^2 - k_1p_1 - k_1p_2 + p_1p_2)],$$
$$\mathcal{M}_{13} = \bar{u}(p_1)\epsilon\!\!\!/_1(p\!\!\!/_1 - k\!\!\!/_1 + m_c)\gamma_\mu J_V \epsilon\!\!\!/_2(p\!\!\!/_3 - k\!\!\!/_2 + m_c)\gamma^\mu u(p_4)/[8(k_1p_1)(k_2p_3)(m_c^2 - k_1p_1 - k_1p_2 + p_1p_2)],$$
$$\mathcal{M}_{14} = \bar{u}(p_1)\gamma_\mu(k\!\!\!/_1 - p\!\!\!/_2 + m_c)\epsilon\!\!\!/_1 J_V \epsilon\!\!\!/_2(p\!\!\!/_3 - k\!\!\!/_2 + m_c)\gamma^\mu u(p_4)/[8(k_1p_2)(k_2p_3)(m_c^2 - k_1p_1 - k_1p_2 + p_1p_2)],$$
$$\mathcal{M}_{21} = \bar{u}(p_1)\epsilon\!\!\!/_1(p\!\!\!/_1 - k\!\!\!/_1 + m_c)\epsilon\!\!\!/_2(p\!\!\!/_1 - k\!\!\!/ + m_c)\gamma_\mu J_V \gamma^\mu u(p_4)/[8(k_1p_1)(kp_1)(m_c^2 + p_3p_4)],$$

$$\mathcal{M}_{22} = \bar{u}(p_1)\epsilon\!\!\!/_1(p\!\!\!/_1 - k\!\!\!/_1 + m_c)\gamma_\mu(k\!\!\!/_2 - p\!\!\!/_2 + m_c)\epsilon\!\!\!/_2 J_V \gamma^\mu u(p_4)/[8(k_1p_1)(k_2p_2)(m_c^2 + p_3p_4)],$$
$$\mathcal{M}_{23} = \bar{u}(p_1)\gamma_\mu(k\!\!\!/ - p\!\!\!/_2 + m_c)\epsilon\!\!\!/_1(k\!\!\!/_2 - p\!\!\!/_2 + m_c)\epsilon\!\!\!/_2 J_V \gamma^\mu u(p_4)/[8(k_2p_2)(kp_2)(m_c^2 + p_3p_4)],$$
$$\mathcal{M}_{31} = \bar{u}(p_1)\gamma_\mu J_V \gamma^\mu(k\!\!\!/ - p\!\!\!/_4 + m_c)\epsilon\!\!\!/_1(k\!\!\!/_2 - p\!\!\!/_4 + m_c)\epsilon\!\!\!/_2 u(p_4)/[8(k_2p_4)(kp_4)(m_c^2 + p_1p_2)],$$
$$\mathcal{M}_{32} = \bar{u}(p_1)\gamma_\mu J_V \epsilon\!\!\!/_1(p\!\!\!/_3 - k\!\!\!/_1 + m_c)\gamma^\mu(k\!\!\!/_2 - p\!\!\!/_4 + m_c)\epsilon\!\!\!/_2 u(p_4)/[8(k_2p_4)(k_1p_3)(m_c^2 + p_1p_2)],$$
$$\mathcal{M}_{33} = \bar{u}(p_1)\gamma_\mu J_V \epsilon\!\!\!/_1(p\!\!\!/_3 - k\!\!\!/_1 + m_c)\epsilon\!\!\!/_2(p\!\!\!/_3 - k\!\!\!/ + m_c)\gamma^\mu u(p_4)/[8(k_1p_3)(kp_3)(m_c^2 + p_1p_2)],$$

$$\mathcal{M}_{41} = \bar{u}(p_1)\not{\epsilon}_1(\not{p}_1 - \not{k}_1 + m_c)\gamma^\mu J_V \gamma^\nu u(p_4) G^{(3)}(k_{2\sigma}, -(p_3+p_4)_\nu, (p_3+p_4-k_2)_\mu)\epsilon_2^\sigma / [8(k_1p_1)(m_c^2 + p_3p_4) \times (m_c^2 - k_1p_1 - k_1p_2 + p_1p_2)],$$

$$\mathcal{M}_{42} = \bar{u}(p_1)\gamma^\mu(\not{p}_1 - \not{k}_1 + m_c)\not{\epsilon}_1 J_V \gamma^\nu u(p_4) G^{(3)}(k_{2\sigma}, -(p_3+p_4)_\nu, (p_3+p_4-k_2)_\mu)\epsilon_2^\sigma / [8(k_1p_2)(m_c^2 + p_3p_4) \times (m_c^2 - k_1p_1 - k_1p_2 + p_1p_2)],$$

$$\mathcal{M}_{45} = \bar{u}(p_1)\gamma^\mu J_V \gamma^\nu(\not{k}_1 - \not{p}_4 + m_c)\not{\epsilon}_1 u(p_4) G^{(3)}(k_{2\sigma}, -(p_1+p_2)_\mu, (p_1+p_2-k_2)_\nu)\epsilon_2^\sigma / [8(k_1p_4)(m_c^2 + p_1p_2) \times (m_c^2 - k_1p_1 - k_1p_2 + p_1p_2)],$$

$$\mathcal{M}_{46} = \bar{u}(p_1)\gamma^\mu J_V \not{\epsilon}_1(\not{p}_3 - \not{k}_1 + m_c)\gamma^\nu u(p_4) G^{(3)}(k_{2\sigma}, -(p_1+p_2)_\mu, (p_1+p_2-k_2)_\nu)\epsilon_2^\sigma / [8(k_1p_3)(m_c^2 + p_1p_2) \times (m_c^2 - k_1p_1 - k_1p_2 + p_1p_2)],$$

$$\mathcal{M}_{51} = \bar{u}(p_1)\gamma^\nu(\not{p}_1 - \not{k} + m_c)\gamma_\mu J_V \gamma^\mu u(p_4) G^{(3)}(k_{1\rho}, k_{2\sigma}, -(k_1+k_2)_\nu)\epsilon_1^\rho \epsilon_2^\sigma / [8(k_1k_2)(k_1k_2 - kp_1)(m_c^2 + p_3p_4)],$$

$$\mathcal{M}_{52} = \bar{u}(p_1)\gamma_\mu(\not{k} - \not{p}_2 + m_c)\gamma^\nu J_V \gamma^\mu u(p_4) G^{(3)}(k_{1\rho}, k_{2\sigma}, -(k_1+k_2)_\nu)\epsilon_1^\rho \epsilon_2^\sigma / [8(k_1k_2)(k_1k_2 - kp_2)(m_c^2 + p_3p_4)],$$

$$\mathcal{M}_{53} = \bar{u}(p_1)\gamma_\mu J_V \gamma^\mu(\not{k} - \not{p}_4 + m_c)\gamma^\nu u(p_4) G^{(3)}(k_{1\rho}, k_{2\sigma}, -(k_1+k_2)_\nu)\epsilon_1^\rho \epsilon_2^\sigma / [8(k_1k_2)(k_1k_2 - kp_4)(m_c^2 + p_1p_2)],$$

$$\mathcal{M}_{54} = \bar{u}(p_1)\gamma_\mu J_V \gamma^\nu(\not{p}_3 - \not{k} + m_c)\gamma^\mu u(p_4) G^{(3)}(k_{1\rho}, k_{2\sigma}, -(k_1+k_2)_\nu)\epsilon_1^\rho \epsilon_2^\sigma / [8(k_1k_2)(k_1k_2 - kp_3)(m_c^2 + p_1p_2)],$$

$$\mathcal{M}_{61} = \bar{u}(p_1)\gamma^\mu J_V \gamma^\nu u(p_4) G^{(3)}(k_{1\rho}, k_{2\sigma}, -(k_1+k_2)_\lambda) G^{(3)}((k_1+k_2)_\lambda, -(p_1+p_2)_\mu, -(p_3+p_4)_\nu)\epsilon_1^\rho \epsilon_2^\sigma / [8(k_1k_2)(m_c^2 + p_1p_2)(m_c^2 + p_3p_4)],$$

$$\mathcal{M}_{62} = \bar{u}(p_1)\gamma^\mu J_V \gamma^\nu u(p_4) G^{(3)}(k_{1\rho}, -(p_1+p_2)_\mu, (p_1+p_2-k_1)_\lambda) G^{(3)}(k_{2\sigma}, -(p_1+p_2-k_1)_\lambda, -(p_3+p_4)_\nu)\epsilon_1^\rho \epsilon_2^\sigma / [8(m_c^2 + p_1p_2)(m_c^2 + p_3p_4)(m_c^2 - k_1p_1 - k_1p_2 + p_1p_2),]$$

$$\mathcal{M}_{64}^{A,B,C} = \bar{u}(p_1)\gamma^\mu J_V \gamma^\nu u(p_4) G^{(4)A,B,C}_{\rho\sigma\mu\nu} a_1^\rho a_2^\sigma / [4(m_c^2 + p_1p_2)(m_c^2 + p_3p_4)],$$

and one has to add expressions corresponding to the interchange of the initial gluons $(k_1, a_1) \leftrightarrow (k2, a_2)$ in $\mathcal{M}_{11-46}$ and $\mathcal{M}_{62}$.

In the above formulas, $G^{(3)}$ and $G^{(4)}$ are related to the standard QCD three- and four-gluon couplings with $G^{(4)}$ being split into three terms possessing different color structure:

$$G^{(3)}(p_\lambda, q_\mu, k_\nu) = ((q-p)_\nu g_{\lambda\mu} + (k-q)_\lambda g_{\mu\nu} + (p-k)_\mu g_{\nu\lambda}), \qquad G^{(4)A}_{\lambda\mu\nu\sigma} = (g_{\lambda\nu}g_{\mu\sigma} - g_{\lambda\sigma}g_{\mu\nu}),$$
$$G^{(4)B}_{\lambda\mu\nu\sigma} = (g_{\lambda\mu}g_{\nu\sigma} - g_{\lambda\sigma}g_{\mu\nu}), \qquad G^{(4)C}_{\lambda\mu\nu\sigma} = (g_{\lambda\nu}g_{\mu\sigma} - g_{\lambda\mu}g_{\nu\sigma}).$$

Explicitly, the color structure of the above matrix elements reads

$$\mathcal{M}^{\rm col}_{11} = (T^a)^\alpha_\zeta (T^c)^\zeta_\xi (T^c)^\xi_\tau (T^b)^\tau_\beta, \qquad \mathcal{M}^{\rm col}_{12} = (T^c)^\alpha_\zeta (T^a)^\zeta_\xi (T^c)^\xi_\tau (T^b)^\tau_\beta, \qquad \mathcal{M}^{\rm col}_{13} = (T^a)^\alpha_\zeta (T^c)^\zeta_\xi (T^b)^\xi_\tau (T^c)^\tau_\beta,$$
$$\mathcal{M}^{\rm col}_{14} = (T^c)^\alpha_\zeta (T^a)^\zeta_\xi (T^b)^\xi_\tau (T^c)^\tau_\beta, \qquad \mathcal{M}^{\rm col}_{21} = (T^a)^\alpha_\zeta (T^b)^\zeta_\tau (T^c)^\tau_\xi (T^c)^\xi_\beta, \qquad \mathcal{M}^{\rm col}_{22} = (T^a)^\alpha_\zeta (T^c)^\zeta_\tau (T^b)^\tau_\xi (T^c)^\xi_\beta,$$
$$\mathcal{M}^{\rm col}_{23} = (T^c)^\alpha_\zeta (T^a)^\zeta_\tau (T^b)^\tau_\xi (T^c)^\xi_\beta, \qquad \mathcal{M}^{\rm col}_{31} = (T^c)^\alpha_\xi (T^c)^\xi_\tau (T^a)^\tau_\zeta (T^b)^\zeta_\beta, \qquad \mathcal{M}^{\rm col}_{32} = (T^c)^\alpha_\xi (T^a)^\xi_\tau (T^c)^\tau_\zeta (T^b)^\zeta_\beta,$$
$$\mathcal{M}^{\rm col}_{33} = (T^c)^\alpha_\xi (T^a)^\xi_\tau (T^b)^\tau_\zeta (T^c)^\zeta_\beta, \qquad \mathcal{M}^{\rm col}_{41} = (T^a)^\alpha_\zeta (T^c)^\zeta_\xi (T^d)^\xi_\beta i f^{cbd},$$
$$\mathcal{M}^{\rm col}_{42} = (T^c)^\alpha_\zeta (T^a)^\zeta_\xi (T^d)^\xi_\beta i f^{cbd}, \qquad \mathcal{M}^{\rm col}_{45} = (T^c)^\alpha_\xi (T^d)^\xi_\tau (T^a)^\tau_\beta i f^{bcd}, \qquad \mathcal{M}^{\rm col}_{46} = (T^c)^\alpha_\xi (T^a)^\xi_\tau (T^d)^\tau_\beta i f^{bcd},$$
$$\mathcal{M}^{\rm col}_{51} = (T^c)^\alpha_\zeta (T^d)^\zeta_\xi (T^d)^\xi_\beta i f^{abc}, \qquad \mathcal{M}^{\rm col}_{52} = (T^d)^\alpha_\zeta (T^c)^\zeta_\xi (T^d)^\xi_\beta i f^{abc}, \qquad \mathcal{M}^{\rm col}_{53} = (T^d)^\alpha_\xi (T^d)^\xi_\tau (T^c)^\tau_\beta i f^{abc},$$
$$\mathcal{M}^{\rm col}_{54} = (T^d)^\alpha_\xi (T^c)^\xi_\tau (T^d)^\tau_\beta i f^{abc}, \qquad \mathcal{M}^{\rm col}_{64A} = (T^c)^\alpha_\xi (T^d)^\xi_\beta f^{abe} f^{cde}, \qquad \mathcal{M}^{\rm col}_{64B} = (T^c)^\alpha_\xi (T^d)^\xi_\beta f^{ace} f^{bde},$$
$$\mathcal{M}^{\rm col}_{64C} = (T^c)^\alpha_\xi (T^d)^\xi_\beta f^{aed} f^{bce}, \qquad \mathcal{M}^{\rm col}_{61} = \mathcal{M}^{\rm col}_{64A}, \qquad \mathcal{M}^{\rm col}_{62} = -\mathcal{M}^{\rm col}_{64B}.$$

Here, the upper and lower greek indices denote the fundamental triplet and antitriplet states, while the latin indices belong to the joint eightfold representation of the $SU(3)_{\rm color}$ group. The initial gluons carry the colors a and b, and the final-state quark and antiquark carry the colors α and β, respectively.

[1] S. P. Baranov, Yad. Fiz. **60**, 1459 (1997) [Phys. At. Nucl. **60**, 1322 (1997)].
[2] A. C. Hearn, Utah University Report No. CP78 Rev. 4/84 (Rand Publishing, Utah, 1984).
[3] L. V. Gribov, E. M. Levin, and M. G. Ryskin, Phys. Rep. **100**, 1 (1983); E. M. Levin and M. G. Ryskin, Phys. Rep. **189**, 268 (1990).
[4] S. Catani, M. Ciafaloni, and F. Hautmann, Phys. Lett. B **242**, 97 (1990); Nucl. Phys. **B366**, 135 (1991).
[5] J. C. Collins and R. K. Ellis, Nucl. Phys. **B360**, 3 (1991).
[6] C.-H. Chang, Nucl. Phys. **B172**, 425 (1980); E. L. Berger and D. Jones, Phys. Rev. D **23**, 1521 (1981); R. Baier and R. Rückl, Phys. Lett. B **102**, 364 (1981); H. Krasemann, Z. Phys. C **1**, 189 (1979); G. Guberina, J. Kühn, R. Peccei, and R. Rückl, Nucl. Phys. **B174**, 317 (1980).
[7] S. P. Baranov, Phys. Rev. D **66**, 114003 (2002).
[8] S. P. Baranov and N. P. Zotov, J. Phys. G **29**, 1395 (2003); A. V. Lipatov and N. P. Zotov, Eur. Phys. J. C **27**, 87 (2003).
[9] S. Eidelman *et al.* (Particle Data Group), Phys. Lett. B **592**, 1 (2004).
[10] E. A. Kuraev, L. N. Lipatov, and V. S. Fadin, Sov. Phys. JETP **45**, 199 (1977); Ya. Balitsky and L. N. Lipatov, Sov. J. Nucl. Phys. **28**, 822 (1978).
[11] M. Ciafaloni, Nucl. Phys. **B296**, 49 (1988); S. Catani, F. Fiorani, and G. Marchesini, Phys. Lett. B **234**, 339 (1990); Nucl. Phys. **B336**, 18 (1990); G. Marchesini, Nucl. Phys. **B445**, 49 (1995).
[12] J. Blümlein, J. Phys. G **19**, 1623 (1993).
[13] M. Glück, E. Reya, and A. Vogt, Z. Phys. C **67**, 433 (1995).
[14] E. Bycling and K. Kajantie, *Particle Kinematics* (John Wiley & Sons, New York, 1973).
[15] G. P. Lepage, J. Comput. Phys. **27**, 192 (1978).
[16] C. Peterson, D. Schlatter, I. Schmitt, and P. Zerwas, Phys. Rev. D **27**, 105 (1983).
[17] P. Cho and A. K. Leibovich, Phys. Rev. D **53**, 150 (1996); **53**, 6203 (1996).
[18] M. Krämer, Nucl. Phys. **B459**, 3 (1996).
[19] A. V. Berezhnoy, V. V. Kiselev, A. K. Likhoded, and A. I. Onishchenko, Phys. Rev. D **57**, 4385 (1998).